Experimental and Numerical Investigation of Injection Rate Shaping in a Small-Bore Direct-Injection Diesel Engine

V. Luckhchoura[1*], F. -X. Robert[1], N. Peters[1], M. Rottmann[2], S. Pischinger[2]
[1]Institute for Combustion Technology
RWTH Aachen University, Aachen, Germany
[2]Institute for Internal Combustion Engines
RWTH Aachen University, Aachen, Germany

This study evaluates the Boot and the Top-hat injection rate shapes at a single high-load point of a single cylinder small-bore direct-injection (DI) Diesel engine using experimental and multidimensional engine simulations results. In experiments, injection rate shapes were generated using CoraRS injector. The simulations were performed using Representative Interactive Flamelet (RIF) model. First, model predictions of cylinder pressure and exhaust emissions are validated against experimental data. The trend seen in heat release rate is primarily attributed to the rate of fuel evaporation. A new method – Two-part analysis – is then used to explain the results of simulations. The analysis shows that lower exhaust Soot and CO emissions in Boot shape are due to their faster oxidation in squish region.

Introduction

Fuel injection rate-shaping is one of the measures used to control fuel-air mixing in the combustion chamber, which results in a specific temporal distribution of fuel for a given injection duration. Several studies are available in the literature on fuel injection rate shaping and its effects on engine combustion and performance [1-2].

In this study, engine performance of two injection rate shapes (Boot and Top-hat profiles) at a single load point is evaluated. Common rail rate shaping (CoraRS) injector was used in experiments for generating injection rate shapes. Experiments were conducted at engine speed of 2400 rpm and for a constant indicated mean effective pressure (IMEP) and NO_X emission. Apart from experimental results, multidimensional engine simulation and Two-part analysis of both rate-shapes are also shown in this paper.

Computational Model

In this study, multidimensional engine simulations were performed using RIF model. The RIF model couples the solution of the laminar flamelet equations to the solution of the turbulent flow and mixing field. Computational Fluid Dynamics (CFD) code solves Navier-Stokes equations, equations describing turbulent quantities like mean turbulent kinetic energy ($\tilde{k}$) and its dissipation rate ($\tilde{\varepsilon}$), and the balance equations for mean and variance of mixture fraction describing the mixing field. The flamelet solution provides all scalars as a function of the mixture fraction at each time step. Thereby turbulent mean values of these scalars in a physical space are then obtained by using the "pre-assumed" shape β-PDF (probability distribution function). For the present work, the multidimensional CFD computer code AC-FluX was used, which is based on Finite Volume methods that employ unstructured, and mostly hexahedral meshes. Further detailed description of the RIF model can be found in references [3, 4].

A mixture of 70 percent n-decane and 30 percent α-methylnaphthalene (liquid volume), the so-called IDEA fuel, was used to simulate Diesel fuel. The complete chemical reaction mechanism for IDEA fuel comprises 519 elementary reactions and 109 chemical species.

Experimental Setup

Experiments were carried out in a 0.45 L single-cylinder test engine whose specifications are summarized in Table 1. Further details on experimental setup and on injection system are given in [2]. Data pertaining to engine operating point for both injection rate shapes is shown below in Table 2.

Swept Volume	450 cm^3
Stroke	88 mm
Bore	81 mm
Compression Ratio	16.10
Injector	CoraRS
Hydraulic Flow Rate	450 cm^3 / 30 s
Hole Numbers	7

Table 1: Single cylinder engine specification

Injection Shape	Fuel mass (mg/cycle)	SOI [° ATDC]	EGR [%]
Top-hat	37.60	-1.5	29.22
Boot	38.16	-2	27.73

Table 2: Engine operating points for Top-hat and Boot injection rate shapes

Numerical Setup

For the CFD simulations, a sector mesh representing 1/7th of the combustion chamber was used by taking advantage of the circumferential symmetry of the centrally located injector equipped with a 7-hole nozzle. The computations started

* Corresponding author: V.Luckhchoura@itv.rwth-aachen.de
Towards Clean Diesel Engines, TCDE2009

from intake valve closure (IVC) at -118° after top dead center (ATDC) and ended at exhaust valve open (EVO) at +120° ATDC. Quantities such as trapped mass, intake pressure and temperature, EGR were all obtained from experimental data. Seven different computational meshes were used throughout the simulation during the piston movement from IVC to EVO. Computational mesh at top dead center is shown in Fig. 1.

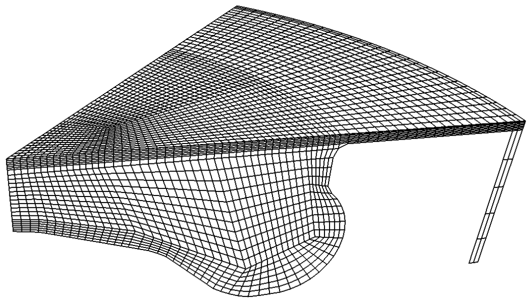

Fig. 1: Computational mesh at top dead center

Comparison between Simulated and Experimentally Measured Data

Fig. 2 shows measured fuel injection rates for Top-hat and Boot shapes. Three stages in injection rate can be seen in Fig. 2: until 2° ATDC injection rate is higher in Boot shape, between 2° and 10° ATDC injection rate is higher in Top-hat, after that injection rate remains higher in Boot shape until the end of injection.

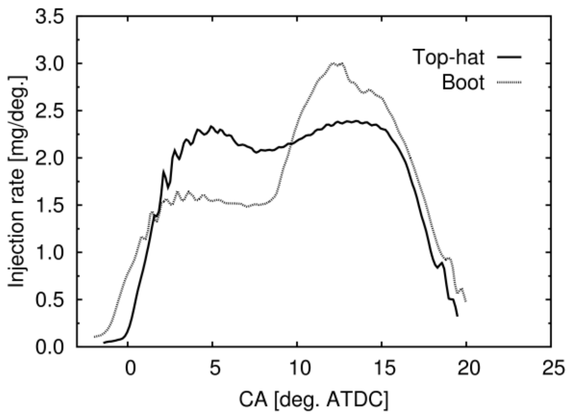

Fig. 2: Measured fuel injection rate for Top-hat and Boot injection rate shapes

Fuel evaporation rate over crank angle for both rate shapes is shown in Fig. 3. Similar to fuel injection rate, three stages in fuel evaporation rate for both rate shapes can clearly be recognized. It is well known that breakup of spray droplets increases with increasing injection velocity, and heat transfer from surrounding gas to droplets is higher in smaller droplets, so does the evaporation rate. Due to initial higher injection rate (and injection velocity) in Boot shape, fuel evaporation starts 1° earlier compared to Top-hat. After 2.5° ATDC analogous to injection rate (see Fig. 3), evaporation rate in Top-hat shape is first higher and then becomes higher in Boot shape.

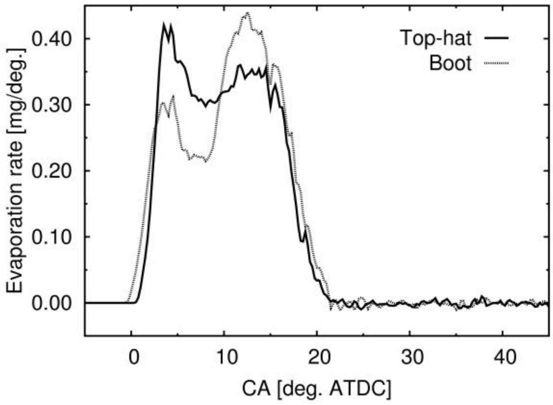

Fig. 3: Fuel evaporation rate for Top-hat and Boot injection rate shapes

Fig. 4 shows comparison of the simulated and experimentally measured cylinder pressure in both rate shapes. Model predicts earlier ignition in Boot shape as also seen in experiments (Fig. 4). For both rate shapes, model-predicted ignition delay is slightly longer. Because of higher evaporated fuel mass during ignition delay, as seen in Fig. 3, peak pressure in Top-hat is higher than in Boot shape.

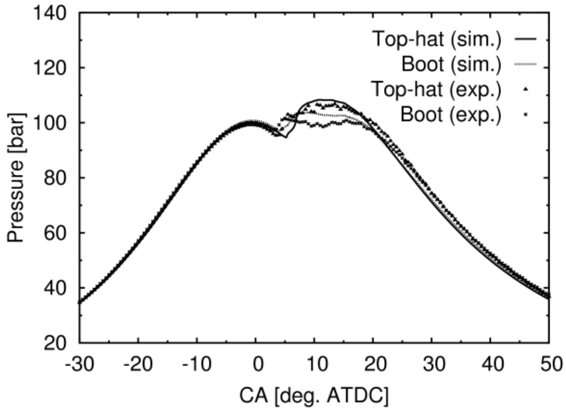

Fig. 4: Comparison between simulated and experimentally measured pressure

Fig. 5 shows simulated heat release rates for both injection rate shapes. Effect of evaporation rate is evident in the heat release for both rate shapes. Earlier start of evaporation in Boot shape shows also early rise in heat release rate. Top-hat shape shows the highest premixed spike in heat release rate due to higher evaporation rate during that period. Higher evaporation rate after 10° ATDC in Boot shape resulted in the highest peak during diffusion-controlled combustion (after the premixed spike in Fig. 5).

Fig. 6 shows the qualitative comparison of simulated and experimentally measured Soot emissions at EVO. Normalized Soot values in Top-hat shape are scaled to one. Similar to experiments, model predicted reduction in Soot emissions at exhaust for Boot shape. Simulated NO_X and CO emissions at EVO were also in good agreement with measured data, though the results are not shown here.

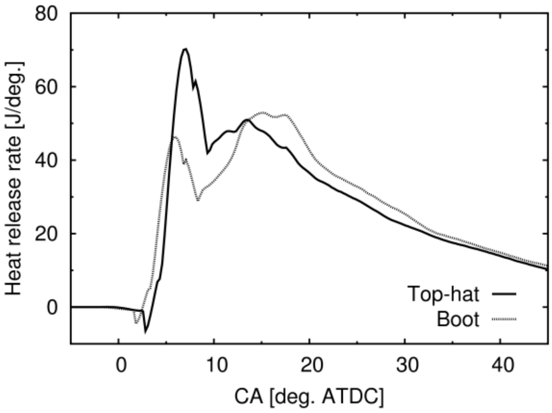

Fig. 5: Simulated heat release rates for Top-hat and Boot injection rate shapes

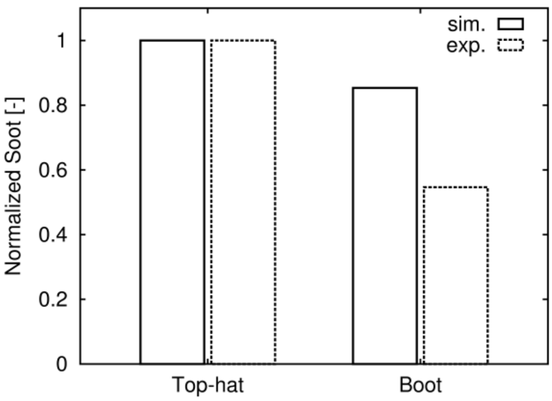

Fig. 6: Comparison between simulated and measured Soot emissions at EVO for both rate shapes

The overall good agreements with experimentally measured data justify the use of model for detailed analysis of simulated data. In the following section, a new approach – Two-part analysis – is introduced and is used to explain trends in Soot emissions.

Two-part Analysis

During simulation of rate shapes, combustion as well as pollutants formation were also noticed in squish region (usually occurs in piston-bowl region). In addition, flow interaction was observed between piston-bowl and squish region. However, magnitudes of pollutants formation and recirculation flow were different in both rate shapes. Fig. 7 shows iso-surfaces of net Soot formation (sum of Soot formation and oxidation) seen in piston-bowl and in squish region. Analysis of the phenomenon occurring within each part and the interactions between the parts due to recirculation flow would reflect the influence of rate shapes. Therefore, Two-part analysis is introduced in this study. It splits combustion chamber in two parts (see Fig. 7). Part 1 is piston-bowl region and part 2 is squish region. Obtained plot of cylinder averaged mean mixture fraction, though not shown here, showed their higher values in part 1 compared to part 2 and the interaction between parts was evident in expansion stroke. Fig. 8 shows net Soot formation over crank angle in both parts for both rate shapes. For both shapes, Soot formation started earlier and was stronger in part 1. Compared to Boot shape, lower peak Soot formation occurred in Top-hat shape (in both parts). However, higher Soot oxidation in Boot shape resulted in lower net Soot formation at EVO.

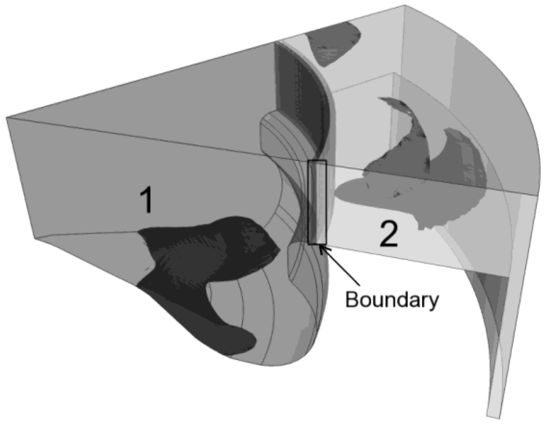

Fig. 7: Simultaneous net Soot formation in piston-bowl and in squish region shown as iso-surfaces; combustion chamber is divided into part 1 and 2

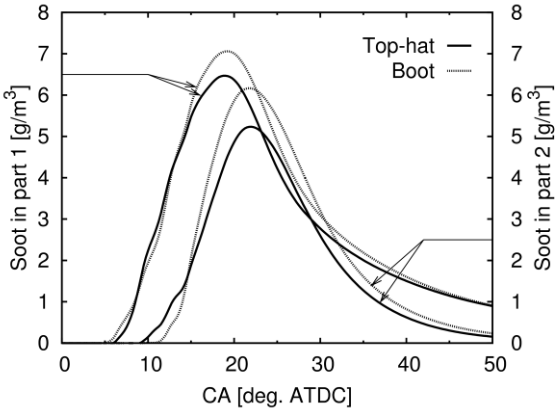

Fig. 8: Simulated net Soot formation in Part 1 and 2, Top-hat and Boot shape

References

[1] O. Kastner, F. Atzler, R. Rotondi and A. Weigand, Evaluation of Injection Strategies for Passenger Car Diesel Engines to meet Euro 6 legislation limits, Thiesel Conference on Thermo- and Fluid Dynamic Processes in Diesel Engines, 2008.

[2] M. Rottmann, C. Menne, S. Pischinger, V. Luckhchoura and N. Peters, Injection Rate Shaping Investigations on a Small Bore DI Diesel Engines, SAE paper 2009-01-0850, 2009.

[3] N. Peters, Turbulent Combustion, Cambridge University Press, 2000.

[4] H. Pitsch, Modellierung der Zuendung und Schadstoffbildung bei der Dieselmotorischen Verbrennung mit Hilfe eines interaktiven Flamelet-Modells, PhD thesis, RWTH Aachen University, Germany, 1997.